Archives of Biochemistry and Biophysics 701 (2021) 108793

Contents lists available at ScienceDirect

Archives of Biochemistry and Biophysics

journal homepage: www.elsevier.com/locate/yabbi

Spectral deconvolution of redox species in the crotonyl-CoA-dependent NADH:ferredoxin oxidoreductase from *Megasphaera elsdenii*. A flavin-dependent bifurcating enzyme

Wayne Vigil Jr. [a], Dimitri Niks [a], Sophie Franz-Badur [a], Nilanjan Chowdhury [b,1], Wolfgang Buckel [b,c], Russ Hille [a,*]

[a] Department of Biochemistry, University of California, Riverside, Riverside, CA, 92521, USA
[b] Max Planck Institute for Terrestrial Microbiology, Marburg, Germany
[c] Fachbereich Biologie and Synmikro, Philipps-Universität, Marburg, Germany

ARTICLE INFO

Keywords:
Electron bifurcation
Flavoprotein
Rapid-reaction kinetics
Electron paramagnetic resonance
Enzyme kinetics
Spectral deconvolution

ABSTRACT

We have undertaken a spectral deconvolution of the three FADs of EtfAB/bcd to the spectral changes seen in the course of reduction, including the spectrally distinct anionic and neutral semiquinone states of electron-transferring and bcd flavins. We also demonstrate that, unlike similar systems, no charge-transfer complex is observed on titration of the reduced *M. elsdenii* EtfAB with NAD^+. Finally, and significantly, we find that removal of the et FAD from EtfAB results in an uncrossing of the half-potentials of the bifurcating FAD that remains in the protein, as reflected in the accumulation of substantial $FAD\bullet^-$ in the course of reductive titrations of the depleted EtfAB with sodium dithionite.

1. Introduction

Bifurcating flavoproteins are a recently discovered class of complex flavoproteins containing multiple redox-active centers [1–4]. They play critical roles in the bioenergetics of anaerobic bacteria and archaea, and utilize an evolutionarily ancient mechanism of energy conservation in which reducing equivalents from a median-potential two-electron donor are delivered individually along separate high- and low-potential pathways to high- and low-potential acceptors in such a way that the overall reaction is thermodynamically favorable. The low-potential reducing equivalents thus generated can be used to drive a variety of intracellular reactions, including ATP synthesis, CO_2 and N_2 fixation, H_2 production, and methanogenesis and acetogenesis, depending on the organism. A subset of bifurcating flavoproteins – including the EtfABCX menaquinone-dependent NADH:ferredoxin oxidoreductase from *Pyrobaculum aerophilum*, the FixABCX ubiquinone-dependent NADH:flavodoxin reductase oxidoreductase, and the EtfAB:bcd crotonyl-CoA-dependent NADH:ferredoxin oxidases from *Megasphaera elsdenii*, *Acidaminococcus fermentans* or *Clostridium difficile* – consists of members that possess an electron-transferring flavoprotein (ETF) component; these and other bifurcating flavoproteins have been the subject of several excellent reviews recently [2–4]. ETF from a variety of both vertebrate and microbial organisms is an αβ dimer with one equivalent of FAD and one of AMP. These simple ETFs do not catalyze bifurcation, but the more complex ETFs such as those enumerated above do. In these latter systems, the ETF component possesses a second equivalent of FAD in place of the AMP found in the simpler ETFs; it is this second FAD that is the site of electron bifurcation. Median-potential electron donors for these bifurcating flavoproteins are typically NADH or NADPH; high-potential acceptors include crotonyl-CoA, caffeyl-CoA, pyruvate, menaquinone and ubiquinone while the low-potential acceptors include ferredoxins and flavodoxins [2–4].

The thermodynamics of flavin-based electron bifurcation are fairly well understood, and take advantage of the fact that the isoalloxazine ring is capable of both one and two-electron processes, with an oxidized quinone state (FAD), a two-electron reduced hydroquinone state ($FADH^-$ at neutral pH), and an intervening one-electron reduced semiquinone state that can exist as either the neutral $FADH\bullet$ or anionic $FAD\bullet^-$. The key feature of a bifurcating flavin is that it has extremely "crossed" half-potentials, with a very low half-potential for the quinone/

* Corresponding author.
E-mail address: russ.hille@ucr.edu (R. Hille).
[1] present address: Institute for Molecular Biosciences Goethe-Universität Frankfurt am Main.

https://doi.org/10.1016/j.abb.2021.108793
Received 24 November 2020; Received in revised form 26 January 2021; Accepted 2 February 2021
Available online 12 February 2021

semiquinone (Q/SQ) couple and very high half-potential for the semiquinone/hydroquinone (SQ/HQ) couple; the semiquinone oxidation state is thus extremely unstable thermodynamically and does not accumulate to any detectable extent in the course of reductive titrations [1,3]. The first electron out of the bifurcating flavin, once reduced, involves the SQ/HQ couple and is high-potential; this leaves behind a very low-potential electron as the thermodynamically unstable semiquinone, which is transferred to the low-potential acceptor.

The bifurcating crotonylCoA-dependent NADH:ferredoxin oxidoreductase, termed EtfAB/bcd (for butyryl-CoA dehydrogenase) from, *e.g.*, *Megasphaera elsdenii*, *Clostridium difficile* and *Acidaminococcus fermentans*, has three equivalents of FAD, two in its ETF component and a third in the butyryl-CoA component, and catalyzes the following reaction [5,6]:

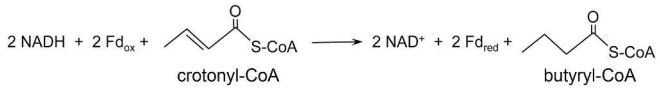

Reduction of the high-potential acceptor crotonyl-CoA and the low-potential acceptor ferredoxin are tightly coupled [1,9,10], ensuring the overall thermodynamic favorability of the reaction. The EtfAB/bcd system is particularly convenient because, while the reduced components are readily reoxidized by O_2, they are not permanently inactivated by O_2. Other systems, particularly those possessing one or more iron-sulfur clusters, are known to be rapidly inactivated on exposure to air.

The reduction potentials of the relevant couples for the EtfAB/bcd complex are [7,8]:

$\Delta E^{NAD+/NADH} = -320$ mV[7]
$\Delta E^{crotonyl-CoA/butyryl-CoA} = -10$ mV[8]
$\Delta E^{Fd/Fd}_{ox\ red} = -420$ mV[8]
$\Delta E^{bifurcating\ FAD}_{Q/HQ} = -279$ mV[7]; $E_{Q/SQ} = -729$ mV[8]*; ESQ/HQ = +171 mV[8]*
$\Delta E^{et\ FAD}_{Q/HQ} = -279$ mV[7]; $E_{Q/SQ} = +81$ mV[7]; $E_{SQ/HQ} = -136$ mV[7]
$\Delta E^{bcd\ FAD}_{Q/HQ} = -19$ mV[7]

N.B. All values are for the *M. elsdenii* system, except the two indicated by an asterisk, which are for the *C. difficile* system.

As mentioned above, the two half-potentials of the bifurcating FAD are highly crossed. In the course of bifurcation, NADH introduces reducing equivalents into the enzyme at the bifurcating FAD of the ETF moiety, reducing it to the hydroquinone $FADH^-$. A first, high-potential electron is transferred to the electron-transferring FAD (et FAD), leaving behind a low-potential electron at the bifurcating FAD (also $FAD\bullet^-$) that is transferred in a thermodynamically downhill manner to the low-potential acceptor ferredoxin ($\Delta\Delta E = {}^-420 - ({}^-729) = {}^+309$ mV) (We note that *in vivo*, the enzyme is likely to have the et FAD already reduced to $FAD\bullet^-$, in which case addition of a second electron yields the hydroquinone which can pass an electron on to the bcd FAD). A second equivalent of NADH again reduces the now reoxidized bifurcating FAD, which again passes a high-potential electron to the et FAD, reducing it now to the hydroquinone, with the remaining low-potential $FAD\bullet^-$ of the bifurcating FAD reducing a second equivalent of ferredoxin. The two electrons in the et FAD are ultimately passed to the enzyme's third FAD, located in the butyryl-CoA dehydrogenase subunit of the enzyme, which reduces crotonyl-CoA to butyryl-CoA ($\Delta\Delta E = {}^-10 - ({}^-19) = {}^+9$ mV). It has been suggested that the thermodynamically uphill initial electron transfer from the bifurcating $FADH^-$ to the et FAD, yielding its $FAD\bullet^-$, serves to keep the system tightly coupled [1]. This step, involving as it does the cleavage of the N5–H bond of the bifurcating $FADH^-$, is necessarily a proton-coupled electron transfer event.

As shown in Fig. 1, *left*, the *C. difficile* enzyme is a tetramer of heterotrimeric protomers, $[EtfAB:bcd]_4$, with the EtfAB units arranged tetrahedrally about a $(bcd)_4$ core [8]. Again, each protomer possesses bifurcating and electron-transferring FADs in the ETF moiety (in green and yellow) and a third FAD in the butyryl-CoA dehydrogenase subunit (in gray). The quaternary structure is arranged as a dimer of dimers, with the bcd subunits of each EtfAB/bcd pair interacting more intimately with one another than with the corresponding subunits of the other pair. Fig. 1, *center*, shows the structure of a single EtfAB/bcd protomer, illustrating the way in which both subunits of EtfAB in fact contribute to each of the two domains of ETF. The et FAD-binding domain of EtfAB (in *red*) is oriented with its C8-methyl group 8.3 Å from the C8-methyl of the bcd FAD (Fig. 1, *right*). The C8-methyl group of the et FAD is more than.

40 Å from that of the bifurcating FAD, although in the structure of the *A. fermentans* EtfAB (lacking the bcd subunit) it is much closer, 18.2 Å, and appears able to move closer still, to 14 Å (considered the maximum distance for efficient electron tunneling) [6]. On the basis of the difference in position of the et FAD domain in these structures, it has been proposed that the et FAD domain undergoes an extensive motion in the course of catalysis, first occupying a position with its FAD proximal to the bifurcating FAD, allowing it to become reduced, and subsequently a position with its FAD proximal to the bcd FAD enabling transfer of reducing equivalents on to bcd for reduction of crotonyl-CoA; this conformational change is thought to be rapid and not rate-limiting to catalysis [8]. The contacts between the bcd subunits of a given $(EtfAB/bcd)_2$ pair may stabilize the overall structure and allow this flexibility. The conformational flexibility of this domain is also seen in simpler, non-bifurcating ETFs [11,12], and is thought to be a general property of this class of flavoproteins.

As a prelude to a detailed kinetic analysis of the *M. elsdenii* EtfAB/bcd

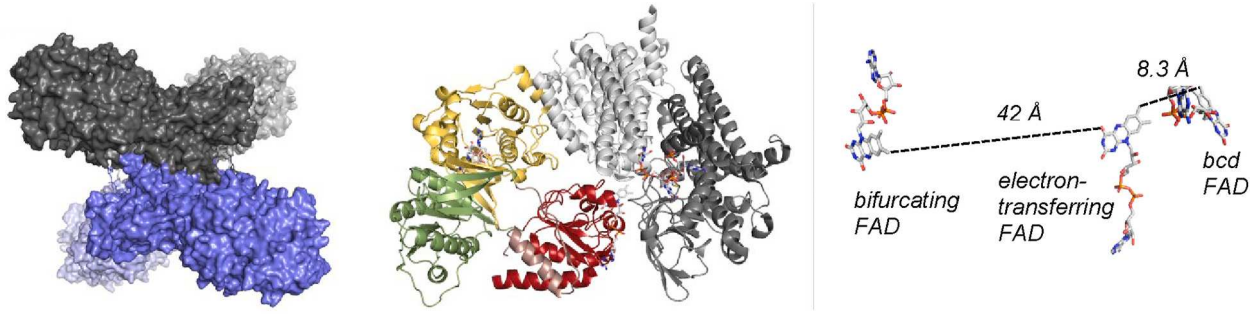

Fig. 1. *Structure of EtfAB/bcd. Left*, the overall topology of the tetrameric *C. difficile* enzyme [8], illustrating how the complex is organized as an $(EtfAB/bcd)_2)_2$ pair of pairs; the upper pair is in dark and light gray, the lower pair in dark and light blue. The tetramer is held together through interactions between the bcd subunits of each protomer. From PDB 5OL2. *Center*, the subunit layout of an individual EtfAB/bcd protomer, with bcd core in *dark gray*; the N-terminal domain of EtfA possessing the bifurcating FAD in *yellow*, its C-terminal domain in *green*, and the domain possessing the et FAD, consisting mostly of EtfB, in *red*. The bcd subunit in the other protomer of the pair is shown in light gray to illustrate how it contributes to the structural stability of the first. *Right*, the disposition of the three equivalents of FAD within one protomer. The orientation is the same as in *center image*.

system, we have undertaken the deconvolution of the spectral contributions attributable to each of the three FADs in the enzyme. We have also further characterized EtfAB in which the et FAD has been removed, demonstrating that the half-potentials of the bifurcating FAD that remains become uncrossed.

2. Experimental

Organisms and Growth Conditions— Construction of the plasmids containing *M. elsdenii* EtfAB (*Mels_2126* + *Mels_2127*) and bcd (*Mels_2128*) genes and a C-terminus Strep II tag derived from pASG-IBA3 (IBA GmbH, Göttingen, Germany), were previously described by Chowdhury et al., 2015 [9]. These were transformed into *E.* coli BL21 cells and grown as previously described, except that the growth medium was changed to Terrific Broth (TB) for both preculture and growth [9]. Precultures were grown in 10 mL of TB with 100 μg/ml ampicillin overnight at 30 °C with shaking at 220 rpm. 100 μg/ml ampicillin was added to 2 L of TB in a 6 L Erlenmeyer flask, inoculated with the preculture and grown for an additional ~6 h at 37 °C and shaking at 180 rpm. When an OD A_{600} of 0.5 was reached, the temperature was reduced to 21 °C and growth continued until an OD of 0.8 was reached. At this point, the cells were induced with 0.1 mM anhydrotetracycline and grown for an additional 24 h. Cells were harvested by centrifugation for 20 min at 5500×*g* at 4 °C, flash frozen in liquid nitrogen and stored at −80 °C until used (typical yields were 11 g cells/L of media).

Purification of M. elsdenii EtfAB — All steps were performed at 0–4 °C and under aerobic conditions unless otherwise stated, using a procedure modified from Chowdhury et al., 2015 [9]. Frozen cells (~22 g wet weight), were thawed and suspended in 0.5–1 g/ml of 50 mM Tris-HCl, 100 mM NaCl, pH 8.0 (Buffer A_1), supplemented with 1 mM NaF (which we have found empirically to be sufficient to prevent proteolysis in the present expression system), 1 mM benzamidine, 0.5 mM PMSF and catalytic amounts of lysozyme and DNase I. The suspension was then incubated for 1 h prior to cell disruption. Cell disruption was performed by 1–2 passages through a French pressure cell at 20,000 psi. Cell debris was removed by centrifugation for 60 min at 42,000×*g*. The crude extract was loaded onto a gravity column containing 6 mL of Strep-Tactin XT Superflow resin (IBA GmbH, Göttingen, Germany) at a rate of 0.5 mL/min, first equilibrated with 5 column volumes of Buffer A_1. The loaded column was then washed with Buffer A_1, flowthrough being monitored spectrophotometrically at 450 nm. Elution began when OD_{280} of the eluate was less than 0.1 (typically after 30 column volumes) with 50 mM Biotin in 50 mM HEPES, pH 7.5 (Buffer B) and was completed after 4 CV's. Purified protein was then exchanged into 50 mM Tris-HCl, 150 mM NaCl, pH 7.5 (Buffer A) and concentrated via Amicon Ultra 4 (Millipore). Because as-isolated EtfAB is known to be partially depleted in the et FAD [7], protein was then incubated ~8 h with 5x molar excess FAD in the dark, after which excess FAD was removed using an 8.3 ml PD-10 (GE Healthcare) column equilibrated in Buffer A. In our hands, protein treated in this way was typically ~90% replete in the et FAD and had the full complement of bifurcating FAD, as reflected in the absorption spectrum. Finally, the protein was aliquoted, flash frozen and stored at −80 °C prior to use.

Purification of M. elsdenii bcd — All steps were performed at 0–4 °C and under aerobic conditions unless otherwise stated. Cell disruption and protein purification were performed as described above for EtfAB, with the exception that the equilibration/wash buffer used was Buffer A. Purified protein was buffer exchanged into Buffer A and concentrated via Amicon Ultra 4 (Millipore). After cell disruption and binding to the affinity column, bcd sometimes turned green, as described previously by Williamson et al., 1982 [13]. To reverse this, the concentrated protein was made anaerobic for 60 min in a procedure described by Niks et al., 2018 [14]. A 5x molar excess of anaerobic sodium dithionite was added to reduce the protein. After 30-min incubation at room temperature to allow for complete reduction, the reaction vessel was opened to air and the protein allowed to re-oxidize before desalting via PD-10, aliquoting and storing as described above. The EtfAB:bcd complex was formed by mixing the separate components in a 1:1 ratio. Unfortunately, no spectral change was associated with complex formation (data not shown), but binding in Buffer A was confirmed in steady-state assays where a stoichiometric excess of ferredoxin became reduced on addition of NADH and crotonyl-CoA [9].

Preparation of Depleted EtfAB — The electron transferring FAD (et FAD) of EtfAB partially dissociates during purification, and prior to use the protein must be reconstituted by incubation with free FAD. In order to deplete the enzyme of the et FAD, incubation and washing with a chaotropic salt was performed similar to the method described by Sato et al., 2003 [15]. First, the enzyme was buffer exchanged into 50 mM K-PO_4, pH 6.0 (Buffer A_2) and concentrated to a minimal volume via Amicon Ultra 4 (Millipore). The concentrated enzyme was then incubated in 50 mM K-PO_4, pH 6.0, 2 M KBr (Buffer B) for 4 h. After washing with Buffer A_2, depletion of the et FAD was confirmed spectrophotometrically. After the initial incubation, the enzyme was washed alternating between Buffers A_2 and B until no more FAD was detectable in the flowthrough (this was typically achieved after four cycles). The protein was finally exchanged into Buffer A, aliquoted and stored as described above.

UV–visible Absorbance Measurements — Static anaerobic titrations and absorbance spectra were performed using a Hewlett-Packard 8452A diode array spectrophotometer equipped with a thermostatted cell holder. Molar extinction coefficients used for each enzyme were: for EtfAB, $\varepsilon_{450} = 21.1\ mM^{-1}cm^{-1}$ and for bcd, $\varepsilon_{450} = 11.8\ mM^{-1}cm^{-1}$ as reported by Sato et al., 2003 [15]. Titrations were performed in an anaerobic quartz sidearm cuvette sealed with a rubber septum (a tonometer was used for stopped-flow experiments) [14]. Samples containing protein and catalytic amounts of glucose oxidase from *Aspergillus niger* (Sigma Type VII, typically 80 nM) and bovine liver catalase (Sigma stock #C-40, typically 8 nM) were made anaerobic using an Ar wet train at room temperature. After anaerobiosis was achieved, 2–10 mM glucose was added from a sidearm of the anaerobic cuvette to continuously scrub the reaction mix of O_2. A reductant (NADH or sodium dithionite) was made anaerobic and then introduced via a Hamilton syringe by piercing the septum seal (the needle interface was sealed with Apiezon N vacuum grease). The initial absorbance change was finished in the mixing time (~5 s) and spectra were obtained after each addition of titrant. Spectra were taken after 5–10 min to ensure complete consumption of titrant and additions continued until the enzyme was fully reduced.

Stable semiquinones (FAD•$^-$ in EtfAB and FADH• in bcd) were observed during the course of titration and were compared with those observed experimentally by Edmonson et al. [16] and spectra generated by Hoben et al. [17]. To observe the maximum amount of FADH•, bcd was exchanged into 50 mM Bis-Tris, 150 mM NaCl, pH 6.0 buffer and titrated with anaerobic sodium dithionite to completion. The replete and depleted EtfAB titrations were carried out in Buffer A with either NADH or sodium dithionite in the same manner. The pure spectra of the FADH• state in the titration of bcd and FAD•$^-$ in replete EtfAB were generated by taking the difference between the spectra of the oxidized enzyme and a point during titration where significant semiquinone accumulated but prior to formation of hydroquinone using SigmaPlot 10 (Systat Software, Inc.). The pure spectra of the hydroquinone states were generated by correcting fully reduced spectra for small contaminations from unreacted enzyme by inspection.

EPR Spectroscopy — FAD•$^-$-containing EPR samples were prepared in Buffer A. FAD•$^-$ was obtained by reducing the replete or depleted EtfAB with sodium dithionite. Optimum amount of FAD•$^-$ was obtained after adding sodium dithionite to 25% reduction of the enzyme (about ~4 e−equivalents); higher levels of reduction led to formation of the hydroquinone species directly or through semiquinone disproportionation as observed in the static titrations. Samples were made anaerobic at room temperature (22 °C) and transferred into argon-flushed, septum-sealed EPR tubes. Sodium dithionite was made anaerobic and added to

the enzyme via Hamilton syringe. Samples were checked spectroscopically to verify semiquinone formation and then immediately frozen in an ethanol/dry ice bath and transferred into liquid nitrogen. EPR spectra were recorded using a Bruker ESP300 spectrometer equipped with a Bruker ER 4119HS high sensitivity X-band cavity and gaussmeter. Temperature was controlled using a Bruker variable temperature unit (set at 150 K) and a liquid nitrogen cryostat. The acquisition software, EWWIN 6.01 (Scientific Software Services) was used to acquire and baseline correct spectra for analysis. For comparison, spectra were converted into *g*-values using the following equation:

$$g = 71.4484 \times \frac{\nu}{B} \quad (1)$$

where ν is in GHz and B is in mT and converted back into mT using the microwave frequency of 9.344. The linewidths of the spectra were compared to the values in Palmer et al., 1971 [18].

3. Results

Spectral deconvolution of the contributions of each FAD in EtfAB/bcd. Despite the presence of three FAD molecules in the EtfAB/bcd complex, deconvolution of the spectral changes attributable to each is in fact more straightforward than might initially be expected for two reasons. First, the oxidized et FAD has a perturbed absorption spectrum that makes it readily distinguishable from either the bifurcating or bcd FAD (Fig. 2, *left*, red spectrum), making it possible to deconvolute the absorption spectra for the bifurcating and et FADs of EtfAB. Our results agree very well with a similar deconvolution performed previously by Sato et al. (2013) [7]. Second, and more importantly, it is possible to deconvolute the contributions of the et FAD•$^-$ and bcd FADH• given their distinct spectroscopic signatures; the two are thus readily distinguishable (the bifurcating FAD is distinct in not forming a stable semiquinone at all, owing to its highly crossed half-potentials). This is important in analyzing future kinetic results as most of the key electron-transfer events of bifurcation are one-electron processes. The bifurcating FAD normally does not form a stable semiquinone owing to its extremely crossed reduction potentials. As shown in Fig. 2 *right*, we have deconvoluted the relevant component spectral changes involved, demonstrating that the spectral changes associated with reduction of each of the three flavins are in fact sufficiently distinct as to allow accurate deconvolution.

The several spectra and difference spectra shown in Fig. 2 are obtained as follows: The spectra of oxidized and fully reduced bcd are obtained with the as-isolated and dithionite-reduced protein, with the FADH• semiquinone (characterized by its extended absorption above 500 nm) essentially quantitatively formed as an intermediate at low pH; the spectral changes associated with formation and decay of the FADH• are obtained straightforwardly by subtraction. The spectrum of oxidized ETF has been deconvoluted by subtracting the spectrum of depleted EtfAB, which gives the absorption spectrum of the bifurcating FAD, from that of the as-isolated protein to give the contribution of the et FAD, which as indicated above is quite distinct from the spectra of either the bifurcating or bcd FAD. The spectral changes associated with formation and decay of the et FAD•$^-$ are obtained from quantitative titrations of replete EtfAB with sodium dithionite, in which the et FAD•$^-$ (with its characteristic absorption band at 370 nm) accumulates essentially quantitatively (correcting for the spectral change associated with reduction of the bifurcating FAD from the quinone to the hydroquinone). It is evident that the difference spectra thus obtained, Fig. 2, *right*, are quite distinct, permitting deconvolution of experimentally obtained spectra and spectral changes.

Absence of a reduced EtfAB:NAD$^+$ charge-transfer complex in the M. elsdenii system. In contrast to other bifurcating flavin systems [19–21], no charge-transfer complexes between reduced EtfAB and NAD$^+$ are observed with the *M. elsdenii* EtfAB. This is illustrated in Fig. 3, where it is seen that addition of NAD$^+$ up to concentrations of 2.5 mM does not elicit any significant long wavelength absorbance in dithionite-reduced EtfAB. The spectral changes that are observed, with increases in absorbance at ~470 nm and ~360 nm, arise from a slight reoxidation of the protein by the added NAD$^+$ due to mass action; the concomitant accumulation of a small amount of NADH is reflected in the increased absorbance at ~360 nm. The oxidized-*minus*-reduced difference spectrum for EtfAB is shown in the inset to Fig. 3, *right*, for comparison. We also find that no long wavelength absorbance is observed on addition of NAD$^+$ to depleted, dithionite-reduced EtfAB (data not shown), but do note that weak long-wavelength absorbance ($\varepsilon_{700} < 1000\ M^{-1}cm^{-1}$) has been observed previously on reduction of the *M. elsdenii* ETF by NADH, although this work was done at pH 5.5 [22].

The bifurcating FAD of depleted EtfAB forms abundant FAD•$^-$. Quite unexpectedly, we observe accumulation of significant amounts of FAD•$^-$ in the course of a reductive titration of depleted EtfAB with sodium dithionite, as reflected in the transient accumulation of absorbance in the 370 nm range in the course of the titration, as shown in Fig. 4 (*left*). Formation of FAD•$^-$ is confirmed by EPR, with a prominent semiquinone spectrum observed with a linewidth of 15 G (Fig. 4, *right*, upper spectrum). The EPR signal seen upon partial reduction of replete EtfAB with sodium dithionite, in which the FAD•$^-$ of the et FAD accumulates, is also shown for comparison (Fig. 4, *right*, lower spectrum). Together with the 370 nm absorbance increase, the narrow linewidth of the EPR signal indicates that it is the anionic rather than neutral semiquinone that is formed [18]. The extremely rapid reduction of the depleted EtfAB by NADH indicates unequivocally that it is the bifurcating FAD that is retained after the KBr treatment, despite the close similarity of the FAD•$^-$ signals arising from the bifurcating and electron-transferring FADs. The

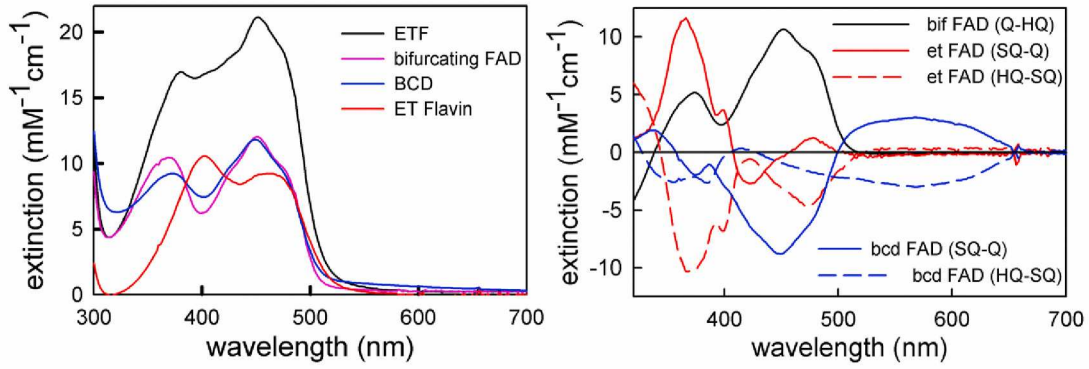

Fig. 2. *Absorption spectra of the component flavins of EtfAB/bcd. Left*, absorption spectra of: replete EtfAB (*black*); EtfAB depleted of the et FAD, yielding the spectrum of the bifurcating FAD (*magenta)*; the et FAD, obtained by subtracting the spectrum of the bifurcating FAD from that for replete EtfAB (*red*); as-isolated bcd (*blue*). *Right*, difference spectra seen for reduction of each flavin (two-electron for the bifurcating FAD, sequential one-electron reduction in the case of the et and bcd FADs).

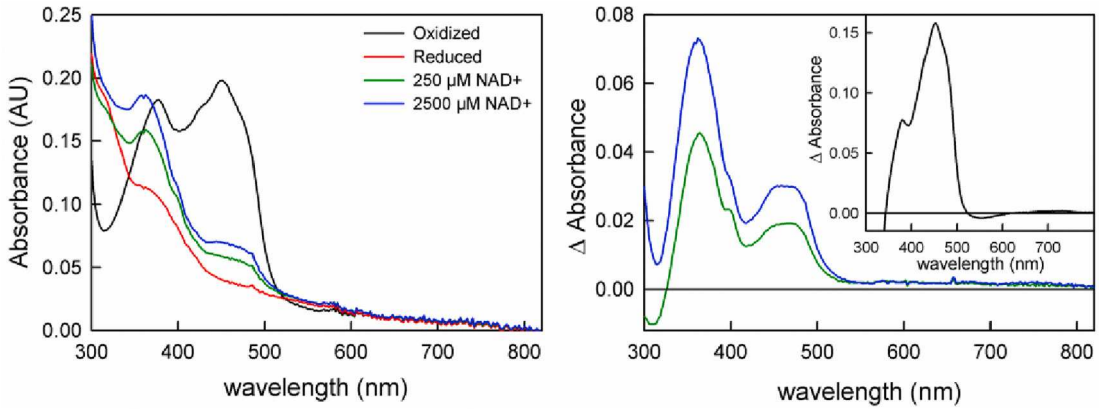

Fig. 3. *The effect of NAD$^+$ on the absorption spectrum of dithionite-reduced EtfAB. Left*, the absorption spectra of oxidized (*black*) and dithionite-reduced (*red*) EtfAB, and the spectra seen after addition of 250 μM (*green*) and 2.5 mM (*blue*) NAD$^+$. *Right*, The difference spectra observed, illustrating the absence of any substantial absorbance above 600 nm, using the same color scheme.

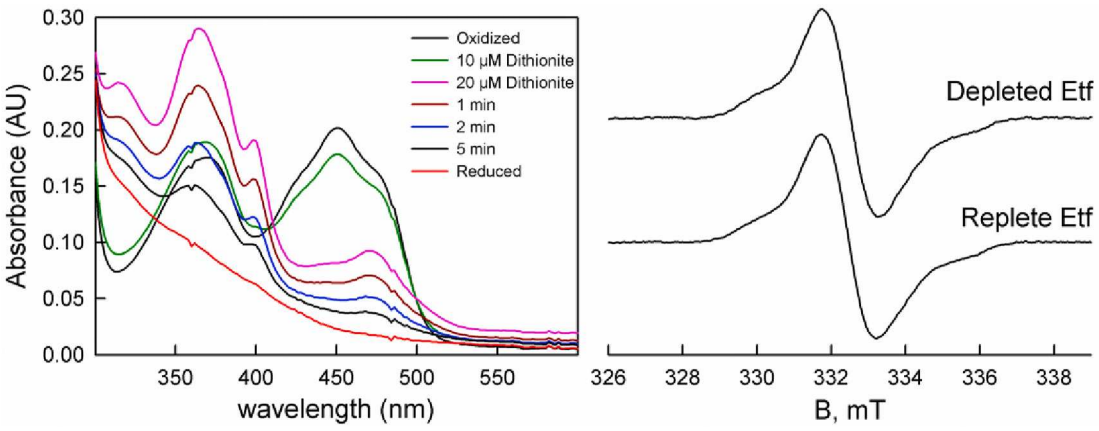

Fig. 4. *Left,* a reductive titration of depleted EtfAB with sodium dithionite. The transient increase in absorbance in the 370 nm region is indicative of accumulation of FAD•$^-$ in the course of the titration. *Right*, X-band EPR of partially reduced, depleted EtfAB, along with the signal seen in the course of a dithionite titration of replete EtfAB, with the signal arising from the FAD•$^-$ of the electron-transferring FAD.

appearance of a strong semiquinone signal attributable to the bifurcating FAD of depleted EtfAB indicates that removal of the electron-transferring FAD results in an uncrossing of the half-potentials of the bifurcating FAD, resulting in the (at least partial) stabilization of the semiquinone oxidation state. The FAD•$^-$ that accumulates upon partial reduction of the depleted EtfAB with dithionite persists indefinitely, and is thermodynamically rather than kinetically stabilized; it does not protonate to the neutral FADH•. The structural basis for the uncrossing of the half-potentials for the bifurcating FAD is under investigation.

It is worth noting that our observation of substantial uncrossing of the bifurcating FADs potentials in the *M. elsdenii* enzyme here differs from the results recently reported by Sucharitakul et al. with the *A. fermentans* enzyme, where no accumulation of either neutral or anionic semiquinone is observed in the course of potentiometric titrations of the depleted EtfAB with sodium dithionite [23].

4. Discussion

The spectral deconvolution undertaken here demonstrates that, perhaps surprisingly, the spectral contributions of the three FADs of EtfAB/bcd are quite distinct, due in large part to the fact that much of the intraprotein electron transfer is taking place in one-electron steps (as reflected in the transient accumulation of semiquinone states) and that the et FAD forms the anionic semiquinone while the bcd FAD forms the neutral species. Deconvolution is further facilitated by the perturbed spectrum of the oxidized et FAD.

It is at first surprising that removal of the et FAD from EtfAB results in the uncrossing of the half-potentials for the bifurcating FAD that remains in the protein, resulting in significant accumulation of the anionic semiquinone in the course of reductive titrations with sodium dithionite. This is particularly the case since strongly crossed half-potentials are widely considered to be a general property common to all bifurcating flavoproteins (including those where the bifurcating FAD is not part of an EtfAB unit) [1,3]. It is important to recognize, however, that there is considerable domain-swapping evident in the crystal structures of both the EtfAB portion of the *C. difficile* EtfAB:bcd complex (*left*) [8] and the isolated *A. fermentans* EtfAB [6]. As shown in Fig. 5, both subunits of EtfAB in fact contribute to the domains in which the two FADs are bound, particularly in the "closed" structure in which the *A. fermentans* protein is found, with the et FAD proximal to the bifurcating FAD. Thus, while the et and bifurcating FADs are frequently referred to in the literature as the α FAD and β FAD, respectively, this is somewhat misleading. The adenosine diphosphate portion of the et FAD does interact primarily with the EtfA (or α) subunit, but its isoalloxazine ring interacts extensively with the body of the EtfB subunit; conversely while the adenosine diphosphate of the bifurcating FAD interacts principally with EtfB (or β), its isoalloxazine ring interacts extensively with the EtfA subunit, at least in the "closed" configuration seen with the *A. fermentans* protein. The differing positions of the domain containing the et FAD is a

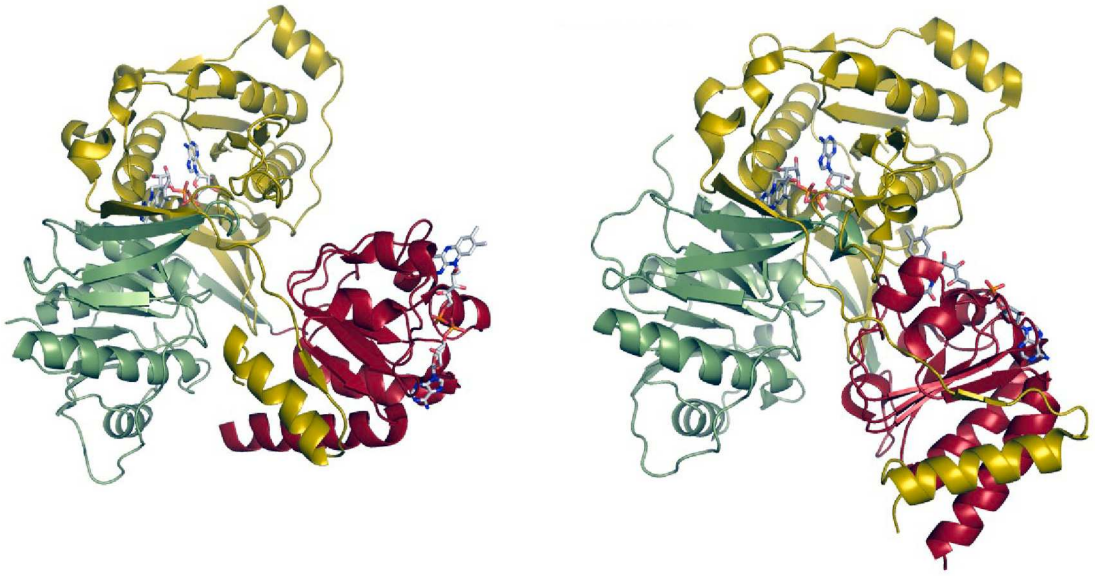

Fig. 5. The structure of EtfAB within the *C. difficile* EtfAB:bcd complex (left)[8], and the isolated EtfAB from Acidaminococcus fermentans[6]. The color scheme and orientation is the same in both cases as in Fig. 1, center: the N-terminal domain of EtfA in green, and it's C-terminal domain in red. The EtfB subunit is in yellow. The two FAD molecules are rendered in stick mode in CPK coloring. The bifurcating FAD is sandwiched between the N-terminal domain of EtfA (green) and the body of EtfB (yellow). The electron-transferring FAD is in a domain that consists principally of the C-terminal portion of EtfA (red), but includes the C-terminal α-helix of EtfB (yellow). It is apparent from a comparison of the two structures that the overall folds of each domain in the two proteins are very similar, as it is for all ETFs, but the orientation of the domain possessing the et FAD is mobile and can assume different orientations relative to the remainder of the protein, as illustrated here. In the *C. difficile* structure at left, the C-terminal domain of EtfA and the et FAD are oriented away from EtfB (yellow) and face the bcd component of the complex (not shown for clarity), while in the A. fermentans structure at right, the C-terminal domain of EtfA (red) and the et FAD pack closely against the body of EtfB (yellow) and in proximity to the bifurcating FAD. The differing orientations are a reflection of the dynamic properties of the domain harboring the et FAD, as mentioned in the text.

manifestation of the dynamic behavior referred to in the Introduction. The domain-swapping evident in the structures provides a structural rationale as to how removal of the et FAD might affect the environment of the bifurcating FAD. The structural basis for the uncrossing of the half-potentials of the bifurcating FAD upon removal of the et FAD is currently being explored crystallographically.

5. Conclusions

The spectral contributions of the three FADs of EtfAB/bcd to the spectral changes seen in the course of reduction have been successfully deconvoluted, taking advantage of the perturbed absorption spectrum of the oxidized et FAD, and the fact that the et and bcd FADs form spectrally distinct anionic and neutral semiquinones.

Unlike other bifurcating flavoprotein systems, the reduced *M. elsdenii* crotonylCoA-dependent NADH:ferredoxin oxidoreductase does not from a long-wavelength-absorbing charge-transfer complex with NAD^+. Finally, and significantly, we find that removal of the et FAD from EtfAB results in an uncrossing of the half-potentials of the bifurcating FAD, as reflected in the accumulation of substantial $FAD^{\bullet -}$ in the course of reductive titrations of the depleted EtfAB with sodium dithionite.

Funding

This work was funded by the US Department of Energy [DE DE-SC0010666] and the National Institutes of Health [GM 135088].

References

[1] G. Herrmann, E. Jayamani, G. Mai, W. Buckel, Energy conservation via electron-transferring flavoprotein in anaerobic bacteria, J. Bacteriol. 190 (2008) 784–791, https://doi.org/10.1128/JB.01422-07.

[2] W. Buckel, R.K. Thauer, Flavin-Based Electron Bifurcation, ferredoxin, flavodoxin and anaerobic respiration with protons (Ech) or NAD+ (Rnf) as electron acceptors: a historical review, Front. Microbiol. 9 (2018), https://doi.org/10.3389/fmicb.2018.00401 article # 401.

[3] W. Buckel, R.K. Thauer, Flavin-based electron bifurcation, A new mechanism of biological energy coupling, Chem. Rev. 118 (2018) 3862–3886, https://doi.org/10.1021/acs.chemrev.7b00707.

[4] W. Buckel, R.K. Thauer, Energy conservation via electron bifurcating ferredoxin reduction and proton/Na+ translocating ferredoxin oxidation, Biochim. Biophys. Acta Bioenerg. 1827 (2013) 94–113, https://doi.org/10.1016/j.bbabio.2012.07.002.

[5] F. Li, J. Hinderberger, H. Seedorf, J. Zhang, W. Buckel, R.K. Thauer, Coupled ferredoxin and crotonyl coenzyme A (CoA) reduction with NADH catalyzed by the butyryl-CoA dehydrogenase/Etf complex from Clostridium kluyveri, J. Bacteriol. 190 (2008) 843–850, https://doi.org/10.1128/JB.01417-07.

[6] N.P. Chowdhury, A.M. Mowafy, J.K. Demmer, V. Upadhyay, S. Koelzer, E. Jayamani, J. Kahnt, M. Hornung, U. Demmer, U. Ermler, W. Buckel, Studies on the mechanism of electron bifurcation catalyzed by electron transferring flavoprotein (ETF) and butyryl-CoA dehydrogenase (Bcd) of *Acidaminococcus fermentans*, J. Biol. Chem. 289 (2014) 5145–5157, https://doi.org/10.1074/jbc.M113.521013.

[7] K. Sato, Y. Nishina, K. Shiga, Interaction between NADH and electron-transferring flavoprotein from *Megasphaera elsdenii*, J. Biochem. 153 (2013) 565–572, https://doi.org/10.1093/jb/mvt026.

[8] J.K. Demmer, N.P. Chowdhury, T. Selmer, U. Ermler, W. Buckel, The semiquinone swing in the bifurcating electron transferring flavoprotein/butyryl-CoA dehydrognenase from *Clostridium difficile*, Nat. Commun. 8 (2017) #, 0.1038/s41467-017-01746-3.

[9] N. Chowdhury, J. Kahnt, W. Buckel, Reduction of ferredoxin or oxygen by flavin-based electron bifurcation in *Megasphera elsdenii*, FEBS J. 282 (2015) 3149–3160, https://doi.org/10.1111/febs.13308.

[10] P.S. Brereton, M.F.J.M. Verhagen, Z.H. Zhou, M.W.W. Adams, Effect of iron-sulfur cluster environment in modulating the thermodynamic properties and biological function of ferredoxin from *Pyrococcus furiosus*, Biochem 37 (1998) 7351–7362, https://doi.org/10.1021/bi972864b.

[11] D. Leys, J. Basran, F. Talfournier, M.J. Sutcliffe, N.S. Scrutton, Extensive conformational sampling in a ternary electron transfer complex, Nat. Struct. Biol. 10 (2003) 219–225, https://doi.org/10.1038/nsb894.

[12] H.S. Toogood, A. van Thiel, J. Basran, M.J. Sutcliffe, N.S. Scrutton, Extensive domain motion and electron transfer in the human electron transferring flavoprotein•medium chain acyl-CoA dehydrogenase complex, J. Biol. Chem. 279 (2004) 32904–32912, https://doi.org/10.1074/jbc.M404884200.

[13] G. Williamson, P.C. Engel, J.P. Mizzer, C. Thorpe, V. Massey, Evidence that the greening ligand in native butyryl-CoA dehydrogenase is a CoA persulfide*, J. Biol. Chem. 257 (8) (1982) 4314–4320. https://www.jbc.org/content/257/8/4314.short.

[14] D. Niks, R. Hille, Reductive activation of CO_2 by formate dehydrogenases, Methods Enzymol. 613 (2018) 277–295, https://doi.org/10.1016/bs.mie.2018.10.013.

[15] K. Sato, Y. Nishina, K. Shiga, Purification of electron-transferring flavoprotein from Megasphaera elsdenii and binding of additional FAD with an unusual absorption spectrum, J. Biochem. 134 (5) (2003) 719–729, https://doi.org/10.1093/jb/mvg199.
[16] D.E. Edmondson, G. Tollin, Semiquinone formation in flavo- and metalloflavoproteins, Radicals in Biochem. Topics in Current Chem. (1983) 109–138, https://doi.org/10.1007/3-540-11846-2_4.
[17] J.P. Hoben, C.E. Lubner, M.W. Ratzloff, G.J. Schut, D.M. Nguyen, K.W. Hempel, A. Miller, Equilibrium and ultrafast kinetic studies manipulating electron transfer: a short-lived flavin semiquinone is not sufficient for electron bifurcation, J. Biol. Chem. 292 (34) (2017) 14039–14049, https://doi.org/10.1074/jbc.m117.794214.
[18] G. Palmer, F. Mueller, V. Massey, Electron paramagnetic resonance studies on flavoprotein radicals, in: H. Kamin (Ed.), Flavins and Flavoproteins, University Park Press, Baltimore, 1971, 132–140.
[19] W. Nitschke, M.J. Russell, Redox bifurcations: mechanisms and importance to life now and at its origin: a widespread means of energy conservation in biology unfolds, Bioessays 34 (2012) 16–109, https://doi.org/10.1002/bies.201100134.
[20] W.W. Metcalf, Classic spotlight: electron bifurcation, a unifying concept for energy conservation in anaerobes, J. Bacteriol. 31 (2016) 146–152, https://doi.org/10.1128/JB.00185-16.
[21] J.W. Peters, C. Lubner, Electron bifurcation makes the puzzle pieces fall energetically into place in methanogenic energy conservation, Chembiochem 18 (2017) 2295–2297, https://doi.org/10.1002/cbic.201700533.
[22] C.D. Whitfield, S.G. Mayhew, Purification and properties of electron-transferring flavoprotein from *Peptostreptococcus elsdenii*, J. Biol. Chem. 249 (9) (1974) 2801–2810.
[23] J. Sucharitakul, S. Buttranon, T. Wongnate, N. Chowdhury, M. Prongjit, W. Buckel, P. Chaiyen, Modulations of the reduction potentials of flavin-based electron bifurcation complexes and semiquinone stabilities are key to control directional electron flow, FEBS J. 287 (2020) 1–19, https://doi.org/10.1111//febs.15343, *early access*.